

Influence of Saturnian moons on Saturn kilometric radiation

J. D. Menietti,¹ J. B. Groene,¹ T. F. Averkamp,¹ G. B. Hospodarsky,¹ W. S. Kurth,¹
D. A. Gurnett,¹ and P. Zarka²

Received 8 February 2007; revised 13 April 2007; accepted 18 May 2007; published 10 August 2007.

[1] Similar to past studies at Jupiter, we conduct an investigation of possible associations of radio emission occurrence probability with the orbital phases of Saturnian moons. We use a new definition of the Saturn longitude system (SLS) based on the results of Kurth et al. (2007). This paper presents results of our findings to date, sampling a large portion of the Radio and Plasma Wave Science (RPWS) instrument data over the frequency range $12 \text{ kHz} < f < 16 \text{ MHz}$. We also investigate the intensity of Saturn kilometric radiation (SKR) as a function of the local time and subsolar longitude. When Titan is near a local time of midnight, there is a significant increase in the occurrence probability of SKR and a diminution of SKR when Titan is near local noon and afternoon. This indicates Titan may play a role in the process of substorm generation at Saturn perhaps due to its large plasma wake. Rhea displays a marginal orbital phase “control” of a subset of the SKR. In the past there have been conflicting reports of the absence of SKR emission at particular local times of Dione. We find no long-term, statistical influence of Dione on SKR occurrence probability. In addition, we find no significant statistical influence of Enceladus or Tethys on SKR occurrence probability.

Citation: Menietti, J. D., J. B. Groene, T. F. Averkamp, G. B. Hospodarsky, W. S. Kurth, D. A. Gurnett, and P. Zarka (2007), Influence of Saturnian moons on Saturn kilometric radiation, *J. Geophys. Res.*, 112, A08211, doi:10.1029/2007JA012331.

1. Introduction

[2] Voyager observations of Saturn kilometric radiation (SKR) revealed emission in the frequency range from a few kHz to about 1.3 MHz, with a peak intensity near 200 kHz [cf. Warwick et al., 1981; Gurnett et al., 1981; Kaiser et al., 1984]. SKR propagates predominantly in the extraordinary mode and has wavelengths in the kilometer band, thus showing great similarity to terrestrial auroral kilometric radiation. The emission is believed to be gyroresonant due to the cyclotron maser mechanism [cf. Kaiser et al., 1984]. A peculiar feature of the Saturn SKR is that it appears to display clock-like periodicity with emission storms occurring when a particular Saturn longitude is near the subsolar point [Warwick et al., 1981; Gurnett et al., 1981]. Kaiser et al. [1981], Kaiser and Desch [1982], and Lecacheux and Genova [1983] have reported that the radio emission sources are in both hemispheres, with the strongest being the northern hemisphere. The northern source appears to be confined to magnetic field lines with footprints in the range $70^\circ < \text{latitude} < 80^\circ$ and $100^\circ < \text{SLS} < 130^\circ$ (Saturn longitude system), and the sources are strongest in the local time range $10 \text{ hours} < \text{LT} < 12 \text{ hours}$. The southern hemisphere source appears to be in the range $-60^\circ < \text{latitude} < -85^\circ$ and 300° to 75° SLS and strongest in the broader range $7 \text{ hours} < \text{LT} < 16 \text{ hours}$. These observations

have never been completely explained, and due to the apparent drifting of the SLS system, it will be important to determine how these observations may have changed. We note that the suggested SKR source regions as well as the UV aurora are at high Saturn latitude, well above the magnetic field line footprints of Enceladus, Tethys, and, usually, Dione and Rhea [cf. Clarke et al., 2005]. The flux tube of Titan, however, should map to high enough latitudes to intercept the SKR source region and the auroral region frequently.

[3] Gurnett et al. [1981] have reported a diminution of SKR with a period of about 66 hours, corresponding to the orbital period of the satellite Dione. This observation was short-lived during the inbound Voyager encounter, when Dione was at orbital phase relative to Voyager of about 270° . Kurth et al. [1981] have suggested the diminution of SKR could be due to refraction of the emission due to a Dione plasma torus. These authors suggested the torus may have a dawn-dusk asymmetry thus explaining the apparent diminution for a Dione phase near dusk only. However, subsequent observations have been not consistent. Desch and Kaiser [1981] reported a Dione control during a later 13-day period of Voyager 1 data, but with Dione at an orbital phase of 30° . Warwick et al. [1982], using Voyager 2 data, reported an SKR increase with an approximate 66-day period, when Dione was at an orbital phase of about 180° . Desch and Kaiser [1981] have reported the Dione control, when present, is strongest for $f < 100 \text{ kHz}$, decreasing up to about 250 kHz.

[4] More recently, Kurth et al. [2005] have reported observations of SKR that correlate with UV observations

¹Department of Physics and Astronomy, University of Iowa, Iowa City, Iowa, USA.

²Observatoire de Paris, Meudon, France.

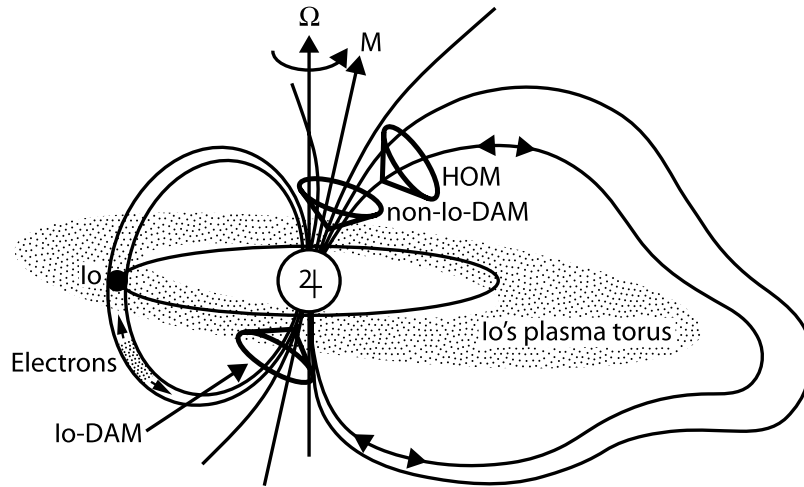


Figure 1. Cartoon showing Io-dependent decametric radiation (DAM) emission at the foot of the Io flux tube. The large-angle emission cone intercepts the ecliptic plane in two general regions separated by about 160 degrees. The non-Io DAM and hectometric radiation (HOM) emissions are also depicted.

of the Hubble Space Telescope. They report that SKR can be associated with bright auroral features just as terrestrial auroral kilometric radiation. In addition, *Farrell et al.* [2005] reported an SKR radio source from an active region in the nightside inner magnetosphere. This is in contrast to many previous reports that the SKR source region is located on the dayside at high latitude.

2. Satellite Control of Radio Emission

[5] Because of their powerful nature and ability to be observed even from ground-based observatories (dating from *Burke and Franklin* [1955]), Jovian decametric radiation ($3 < f < 40$ MHz) has been the most studied planetary radio emission. The correlation between the orbital phase of Io and the occurrence of decametric radiation (DAM) storms [*Bigg*, 1964] marked the beginning of an increasingly intense study of the source location and generation mechanism for DAM emission. Subsequent studies have led to the eventual development of the Jovian longitude-Io phase plots and the familiar nomenclature: Io-A, Io-B, Io-C, and Io-D “sources.” These plots are constructed by plotting the orbital phase of Io versus system III longitude with the radio emission occurrence probability or total wave power color-coded. Excellent descriptions of the Voyager PRA observations can be found in the work of *Warwick et al.* [1979a, 1979b] and *Boischot et al.* [1981], and a thorough review of the spectral phenomenology was presented by *Carr et al.* [1983]. The occurrence of emission for ranges of Io orbital phase centered near $\sim 250^\circ$ and $\sim 80^\circ$ is believed to be due to cyclotron resonant emission at large wave normal angles in a hollow emission cone [cf. *Goldstein and Goertz*, 1983; *Menietti et al.*, 1987; *Wilkinson*, 1989]. We show a cartoon indicating Io-dependent DAM and non-Io DAM and hectometric emission (HOM) in Figure 1. The intersection of the emission cone with the observer in the ecliptic plane produces emission that appears dependent (“controlled”) by the orbital phase of Io.

[6] A variety of mechanisms have been proposed for the electromagnetic interaction of Io and the Jovian magneto-

sphere. *Goldreich and Lynden-Bell* [1969] proposed a unipolar induction electric field across Io producing a current loop closing in Jupiter’s ionosphere. *Neubauer* [1980] has modeled the generation of large-amplitude Alfvén waves that propagate from Io to the ionosphere of Jupiter. The current carried by these waves could be on the order of 10^6 amps. *Crary* [1997] has argued for the generation of electrostatic electric fields parallel to the ambient magnetic field. *Mauk et al.* [2002] and *Ergun et al.* [2002] have suggested a static electric field with an upward and downward current system along the Io flux tube. *Su et al.* [2003] have used a Vlasov code to model such a system and suggest that a 30 keV potential drop along the Io flux tube is consistent with the observations.

[7] The interaction of Titan with the Kronian magnetosphere is different than that of Io with the Jovian magnetosphere. The Alfvén wings of Titan as discussed by *Neubauer et al.* [1984, 2006] are much weaker than those of Io and may not support strong currents to the Kronian ionosphere. The influence of Titan on the magnetosphere of Saturn is not insignificant, however. The flow wake is known to be large in extent ($> 20 R_T$) [cf. *Ma et al.*, 2006] with a significant mass-loading factor ($Q \sim 5 \times 10^{25}/s$) (compare to $Q \sim 10^{27}/s$ for Enceladus and the inner icy satellites) [cf. *Neubauer et al.*, 1984; *Hansen et al.*, 2005; *Ma et al.*, 2006]. All of these latter authors model an extensive flow and ion pick-up wake for Titan. *Sittler et al.* [2006] show that Titan is the source of a large atomic nitrogen torus surrounding Saturn for $L < 20$. This cloud in turn is the source of keV pickup ions [*Hartle et al.*, 2006]. The orbit of Titan at $20.22 R_s$ allows it to come in contact with the magnetopause perhaps 20% of the time as indicated in the studies of *Arridge et al.* [2006, Table 2].

[8] In this paper we report radio wave observations ordered with respect to a new Saturn longitude system based on the results of *Kurth et al.* [2007]. We will present observations which indicate “control” of SKR relative to local time for Titan and possibly to orbital phase for Rhea. We find no evidence for Dione, Enceladus, or

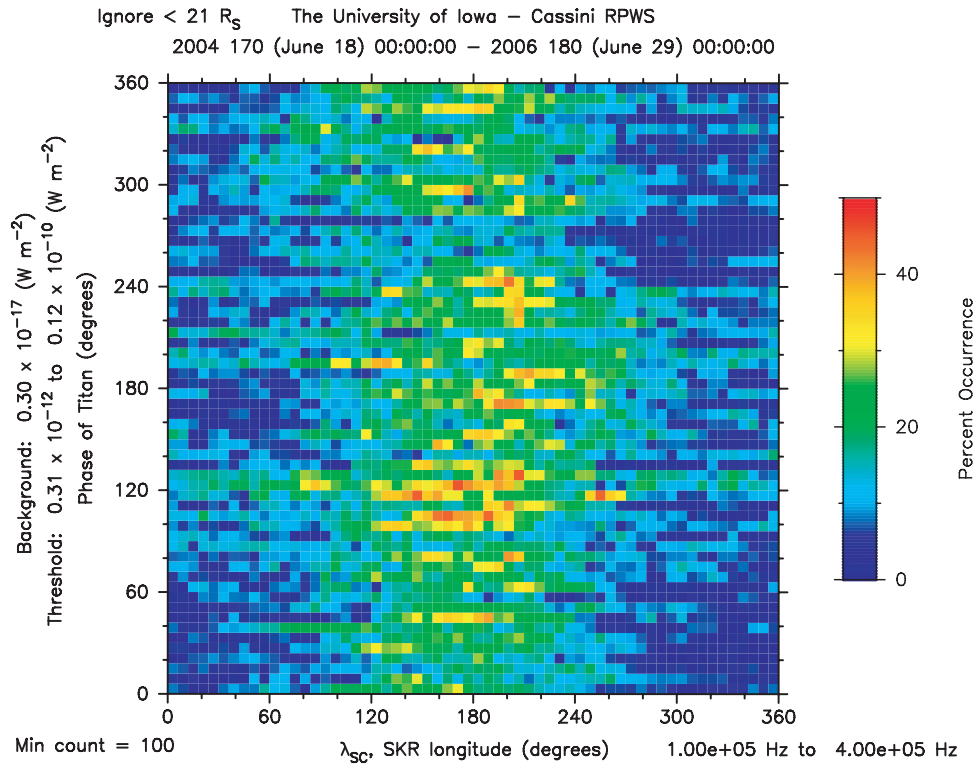


Figure 2. Summary plot in the frequency range $100 \text{ kHz} < f < 400 \text{ kHz}$, for data obtained over the period from 18 June 2004 to 29 June 2006. The orbital phase of Titan is plotted versus SKRLS with occurrence probability of SKR color-coded according to the color bar at right.

Tethys long-term control relative to moon orbital phase or local time.

3. Instrumentation

[9] The Cassini Radio and Plasma Wave Science (RPWS) instrument measures oscillating electric fields over the frequency range 1 Hz to 16 MHz and magnetic fields in the range 1 Hz to 12 kHz [cf. *Gurnett et al.*, 2004]. The instrument uses three electric field antennas and three orthogonal magnetic search coil antennas, providing a direction-finding capability. There are five receiver systems: the high-frequency receiver (HFR) covering 3.5 kHz to 16 MHz; the medium-frequency receiver (MFR) covering 24 Hz to 12 kHz; a low-frequency receiver (LFR) covering 1 Hz to 25 Hz; a high-resolution wideband receiver that covers two frequency bands, 60 Hz to 10.5 kHz and 800 Hz to 74 kHz; and a five-channel waveform receiver with two bandwidths, 25 Hz and 2.5 kHz. The data presented in this study utilize the HFR and MFR exclusively.

4. Observations

[10] To study the influence of Saturnian satellites on radio emission, we investigate occurrence probability of radio emission versus satellite orbital phase and the new SKR longitude system which we refer to as “SKRLS.” Orbital phase is defined relative to superior conjunction with the spacecraft. The SKRLS system has been described in some detail by *Kurth et al.* [2007] and is a variable period system, locked relative to the period of the Saturn kilometric

radiation. We have examined the RPWS data in four separate frequency ranges, 12–100 kHz, 100–400 kHz, 400 kHz to 1 MHz, and 1–16 MHz. These ranges of frequency were chosen to overlap the SKR frequency range and to avoid most of the narrowband kilometric emission tones that are observed for $f < 10 \text{ kHz}$. We present results only for the second frequency range which shows the most significant effects. We evaluate the mean intensity over successive 1-min time intervals for the specified frequency range. A threshold power level is determined for each 10-day period as twice the average of the mean values.

[11] We analyze data obtained during the period 18 June 2004 to 29 June 2006. During this time period the orbit varied considerably. Prior to about day 340, 2004, Cassini orbited with an inclination of about -17 degrees. From this date to about day 109, 2005, the inclination was generally less than about -5 degrees. Between day 109 and day 245, 2005, the inclination varied from -10 to -15 degrees, but after day 250, 2005, the inclination was near zero. The orbit apoapsis has also been precessing clockwise in local time, and after day 300, 2005, the orbit precessed rather rapidly so that the apoapsis moved from the morning sector through the postmidnight sector.

[12] Figure 2 is a summary plot of the results in the frequency range $100 \text{ kHz} < f < 400 \text{ kHz}$ measured by the RPWS for the data period shown. The plot shows data sorted relative to the orbital phase of Titan. The bin size is $6^\circ \times 6^\circ$. The occurrence probability (OP) is defined as the ratio of the number of times a signal was detected above the threshold level divided by the total number of measurements within the $6^\circ \times 6^\circ$ bin and the frequency range. We

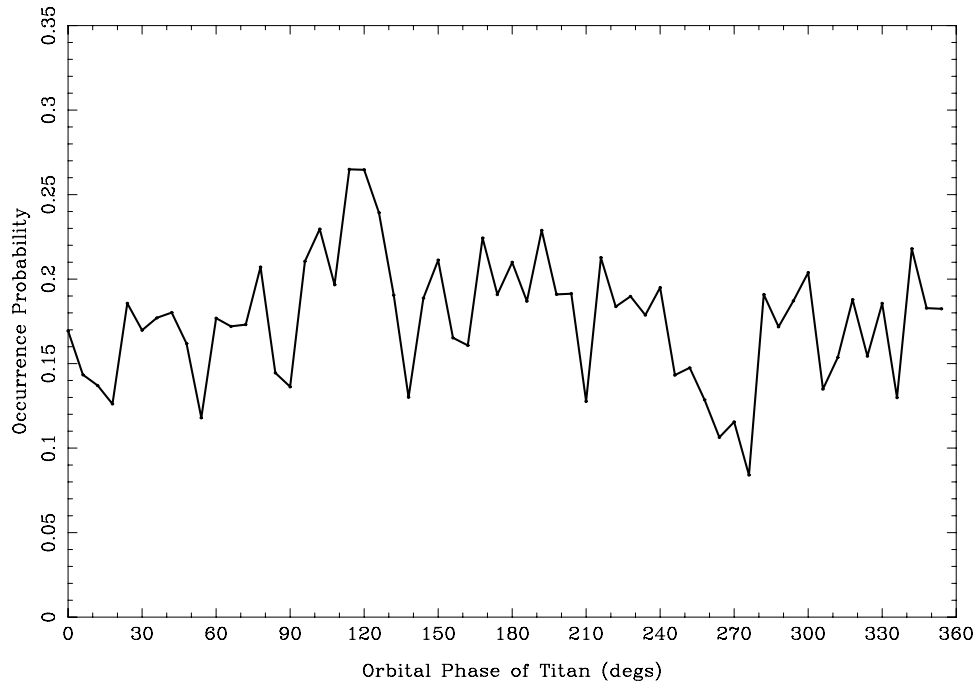


Figure 3. Plot of the occurrence probability (OP) versus Titan orbital phase. The OP is averaged over the range, $72^\circ < \text{SKRLS} < 270^\circ$. Note the peak near 120° and the valley near 275° .

have restricted the data to radial distances greater than the orbit of Titan. Seen in this figure is a significant increase in occurrence probability for Titan orbital phases centered near 120° . In Figure 3 we plot the occurrence probability versus Titan orbital phase, but we have averaged the OP over the range, $72^\circ < \text{SKRLS} < 270^\circ$. Note the peak near 120° and the valley near 275° . The source of this asymmetry in radio emission relative to orbital phase is made clearer if we further examine the dependence of OP on the local time (LT) of Titan. In Figure 4 we plot Titan LT versus the SKR longitude (SKRLS) of the subsolar point (which we call Saturn subsolar longitude or SSSL) with the OP color-coded as before. Note how the OP is enhanced for the range of $21 \text{ hours} < \text{LT} < 3 \text{ hours}$, with a smaller peak centered near 9 hours. These regions are shown in Figure 5 where we plot OP averaged over the range $20^\circ < \text{SSSL} < 180^\circ$ versus Titan LT. Plots 2–5 indicate that SKR is enhanced while Titan is near orbital phase 120° and simultaneously in the magnetotail near LT of midnight. We can understand these two constraints if we further note that the orbits of Cassini during the data collecting period were almost all in the morning sector (with the apoapsis approximately centered near 8–9 hours of local time), precessing in the later months into and through the postmidnight sector. We show a plot of a subset of Cassini orbits in Figure 6. When Titan is near local times of premidnight and postmidnight, Cassini would observe Titan near an orbital phase of 90° – 120° . When Titan is in the range 8–10 hours of local time, it is generally in line with the Cassini spacecraft and Saturn. Thus Cassini may observe an enhancement of SKR emission because some radio emission from sources near Saturn along the Titan flux tube is beamed in the direction of Titan. This also explains the increase in OP for Titan orbital phases near 180° (inferior conjunction) seen in Figure 2.

[13] We investigate this idea by examining a limited dataset during a time when the Cassini orbits were confined to essentially the morning sector (from day 170, 2004, to day 300, 2006). In Figure 7 we show a spectrogram of local time versus SSSL with OP color coded for this limited dataset. In Figure 8 we plot the averaged OP over the range $0 < \text{SSSL} < 200^\circ$. We note that the occurrence probabilities are higher than in Figures 4 and 5, indicating a relatively active period, and the enhancement near 8–10 hours is larger and quite distinct. This is expected if the SKR emission from a source near cyclotron resonance along the Titan flux tube is beamed at large wave normal angle approximately in the direction of Titan with Titan approximately in the same meridian.

[14] We have processed the data shown in Figure 5 a bit more by dividing the range of local times into bins of first 0.8 hours and then 2.0 hours. We then average the occurrence probabilities within these bins for the same range of SSSL as in Figure 5. The results are plotted in Figure 9 with the 0.8 hour (2.0 hour) bin shown in dashed (solid) line. These curves more clearly show the main peak near LT of 1 hour with secondary peaks near 21 hours and 9 hours and the broad null centered near 15 hours LT. We have performed a large-sample population test (z-test) on these data as described by *Mendenhall* [1987] and presented in a similar context for Jovian radio emission data by *Higgins et al.* [2006]. The comparison of two samples of data with normal distributions, or in our case bins of occurrence probabilities, is given by

$$z = \frac{\mu_1 - \mu_2}{\sqrt{\frac{\sigma_1^2}{n_1} + \frac{\sigma_2^2}{n_2}}} \quad (1)$$

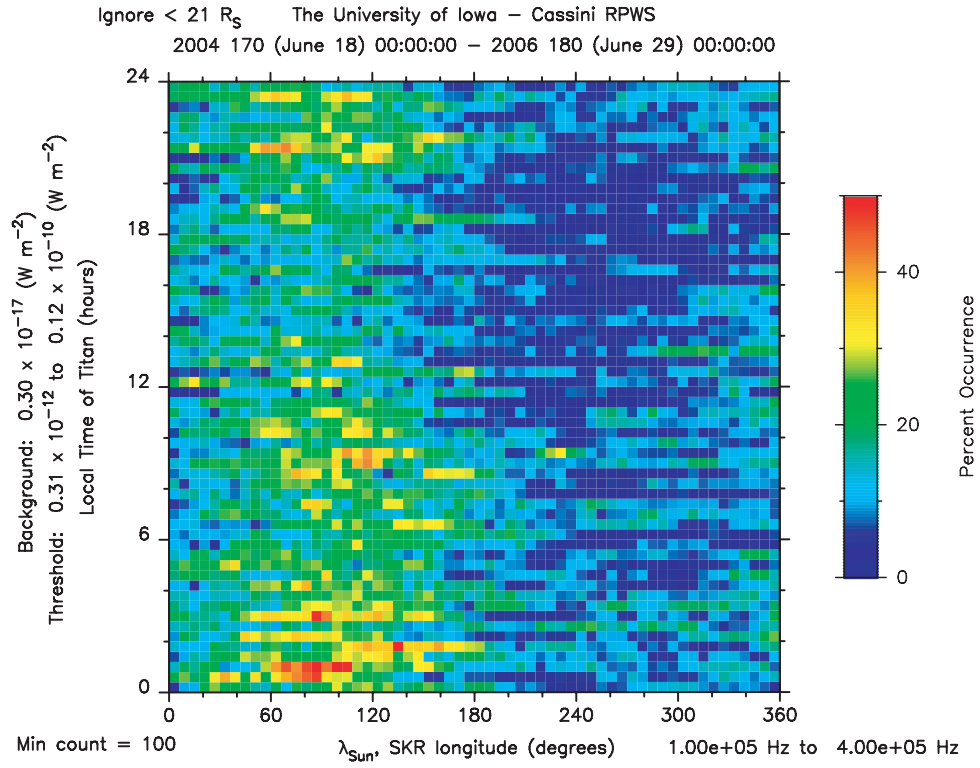


Figure 4. Plot of Titan local time (LT) versus the longitude (SKRLS) of the subsolar point (SSSL) with OP color-coded. OP is enhanced for the range of 21 hours < LT < 3 hours, with a smaller peak centered near 9 hours.

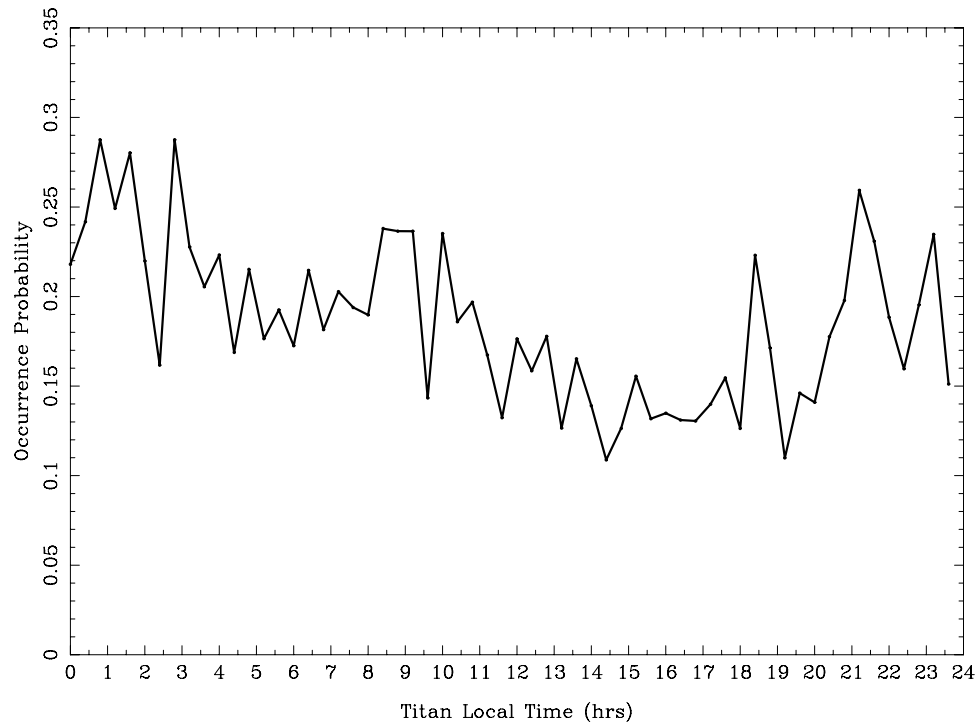


Figure 5. Plot of OP averaged over the range $20^\circ < \text{SSSL} < 180^\circ$ versus Titan LT.

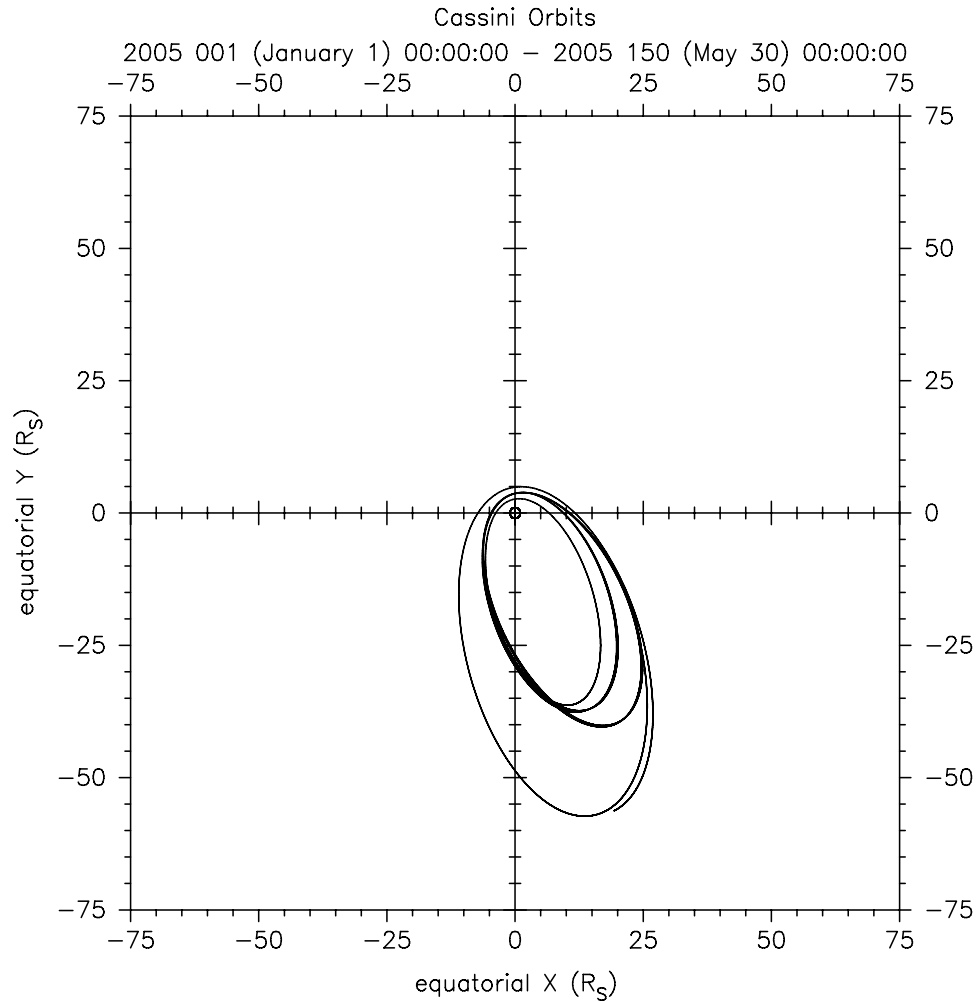


Figure 6. Orbit of Cassini for the 150 day time period 1 January 2005 to 30 May 2005 in equatorial coordinates. The Sun is in the +X direction. During the data-collecting period the majority of orbits were in the morning sector, precessing in the later months into the postmidnight sector.

where μ_1 is the mean value of OP for the subject bin and μ_2 is the mean value of OP for any other bin. Here $\sigma_{1,2}$ and $n_{1,2}$ are the standard deviations and number of data points for those bins, respectively. For the case of bins of size 2 hours LT, each bin contains 135 values. We define the subject bin to be bin 1, centered near the peak at a local time of 1 hour. For the peak OP of this bin to be statistically significant at the 95% confidence level requires that $z > 2$. By comparing z calculated independently with respect to each of the other bins, we find that the smallest value of z is 3.035, and this value results from comparing bin 1 with the adjacent bin. We conclude that the peak observed near a local time of 1 hour is statistically significant.

[15] The data also indicate a range of SKRLS in which the occurrence probability appears to be enhanced (from about 70° to 270°), i.e., a radio emission active zone. However, we believe this zone in SKRLS is also due to the clock-like periodicity of the Saturn emission. Because the orbits of Cassini have not precessed much during the time of the data collection of Figure 2, the appearance of an active zone in SKRLS might be masked by emission that is regularly more active when a specific range of SKRLS is near a local time of 12 hours, as reported in the past [cf.

Gurnett *et al.*, 1981; Warwick *et al.*, 1981]. We will have to wait until later in the Cassini mission, when the apoapsis of the orbit precesses clockwise around Saturn to investigate whether or not a Saturn active zone in SKRLS exists.

5. Results for Other Moons

[16] We have also examined occurrence probability as a function of local time and moon orbital phase for Enceladus, Tethys, Dione, and Rhea. While there are some indications of possible influences on SKR for Enceladus, the results were not conclusive and are not presented. No influence on SKR is observed for Tethys.

[17] We have carefully examined the possible influence of Dione on the occurrence probability of SKR for the lowest two ranges of frequency (12–100 kHz and 100–400 kHz). We find no significant increase or decrease (diminution) of occurrence probability of SKR for any local time or orbital phase. These observations are long-term, statistical studies and do not preclude short-term effects as have been observed in the past.

[18] In Figure 10 we present the data sorted for the orbital phase of Rhea in the same format as Figure 2. For these data

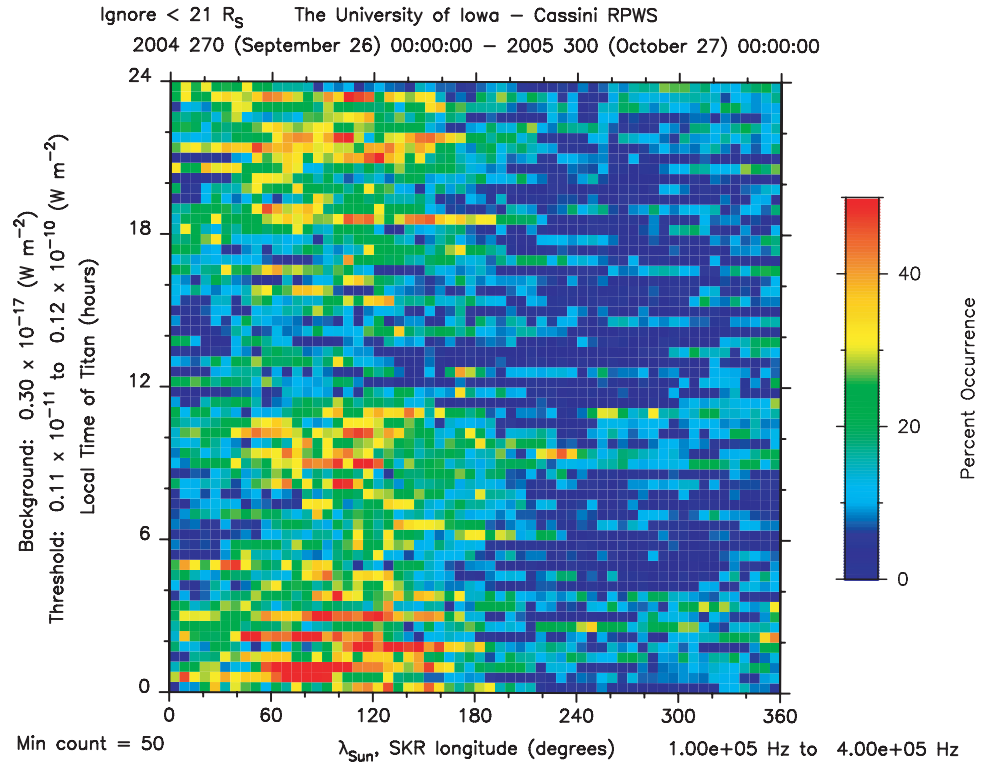


Figure 7. Plot of Titan LT versus SSSL with OP color-coded. Here we have limited the dataset to dates day 270 of 2004 to day 300 of 2006, when the orbit of Cassini is confined to essentially the morning sector.

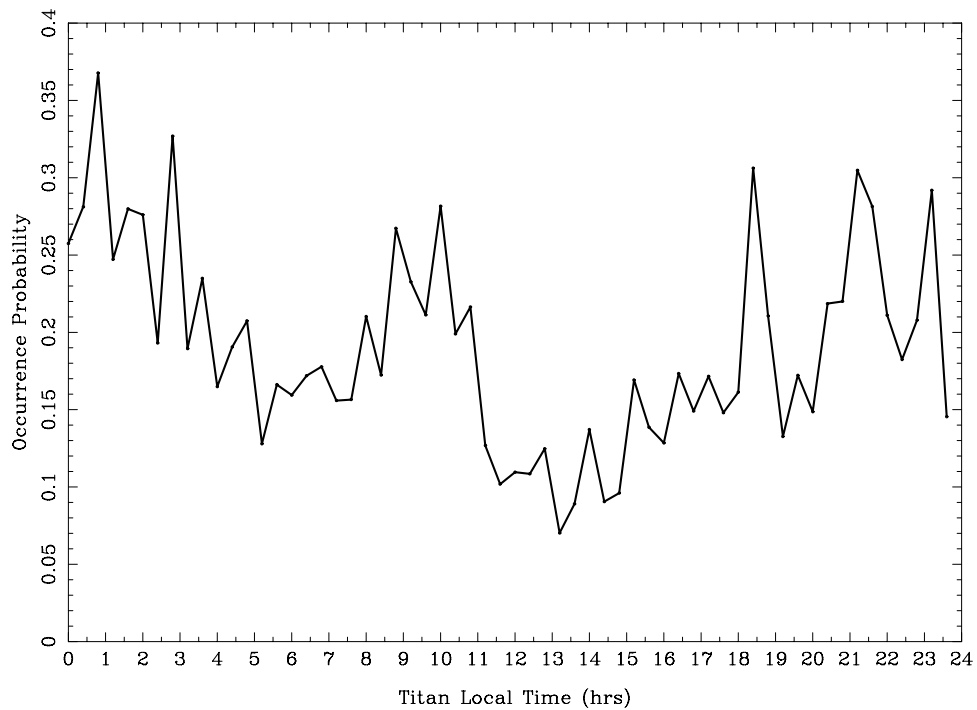


Figure 8. Plot of OP averaged over the range $0^\circ < \text{SSSL} < 200^\circ$ versus Titan LT.

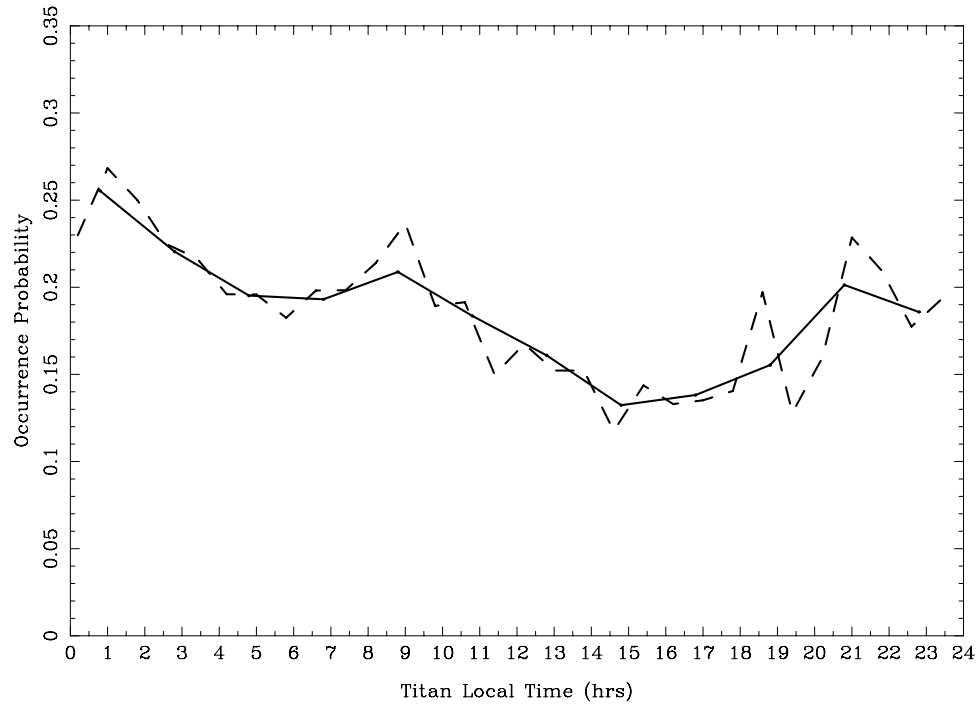


Figure 9. Plot of OP averaged over the range $20^\circ < \text{SSSL} < 180^\circ$ versus Titan LT, as in Figure 4, but now the OP is averaged within larger bins of LT. The dashed (solid) curve is for a LT time bin of 0.8 (2.0) hours.

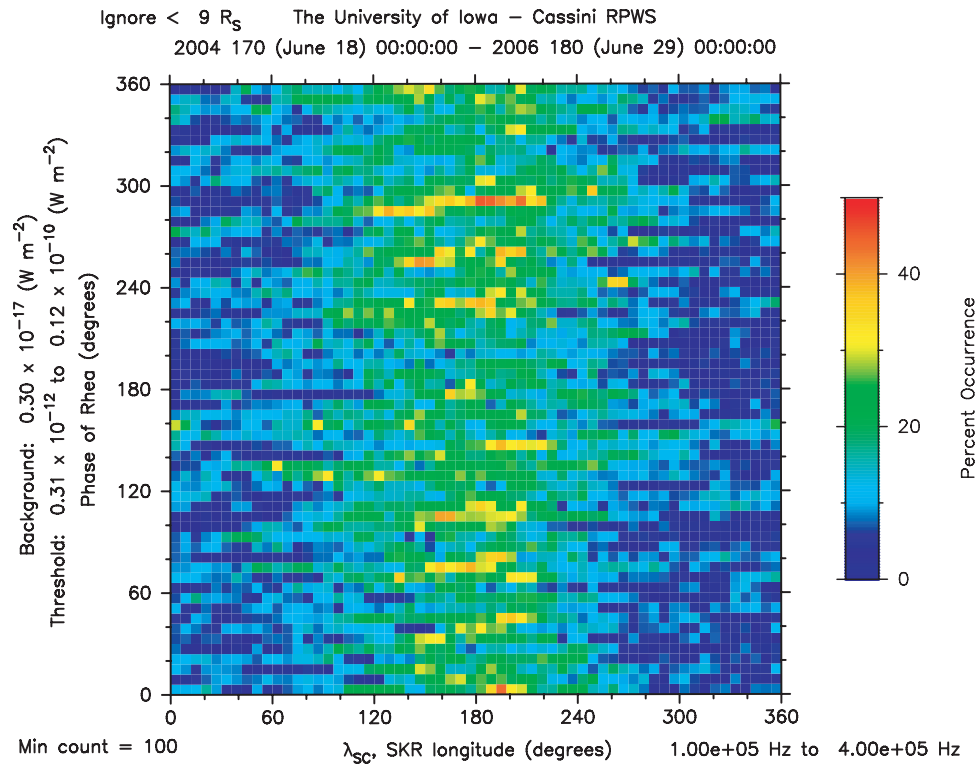


Figure 10. Occurrence probability data sorted for the orbital phase of Rhea in the same format as Figure 1. For these data we see an enhancement in occurrence probability over a narrow range of Rhea orbital phases from about 280° to 295° .

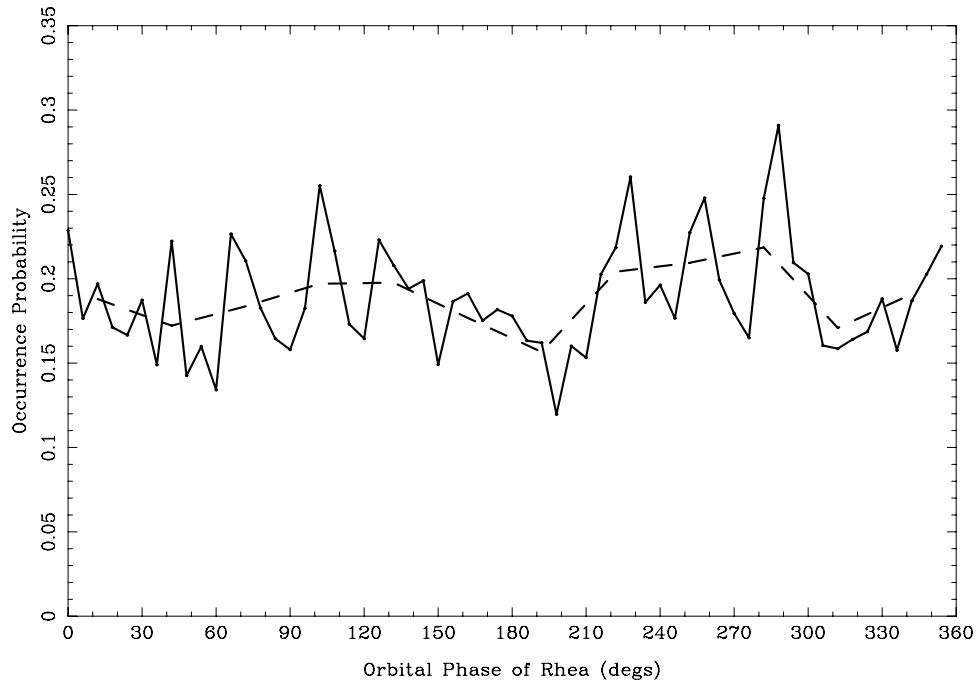


Figure 11. We plot OP averaged over $100^\circ < \text{SKRLS} < 240^\circ$ versus orbital phase. The solid curve (dashed curve) is for a bin size of 6° (30°) in orbital phase of Rhea.

we see a marginally significant enhancement in occurrence probability over a narrow range of Rhea orbital phases from about 280° to 295° . The signature is also seen in the solid curve of Figure 11 where we plot OP averaged over $100^\circ < \text{SKRLS} < 240^\circ$ versus orbital phase. However, Figures 12

and 13, which show the corresponding plots with respect to the local time of Rhea and SSSL, do not indicate a significant enhancement at a particular local time, in contrast to the results for Titan. Similar to the analyses for Titan in Figure 9 we have reprocessed the data of Figure 11 by

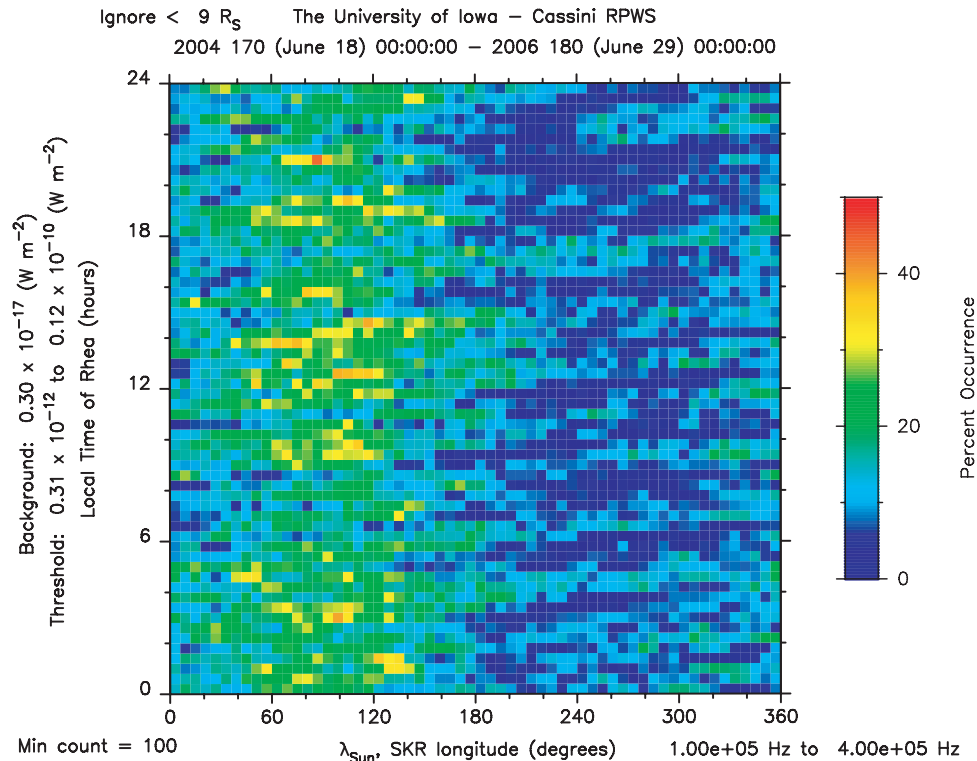


Figure 12. Plot of Rhea LT versus SSSL with OP color-coded as before.

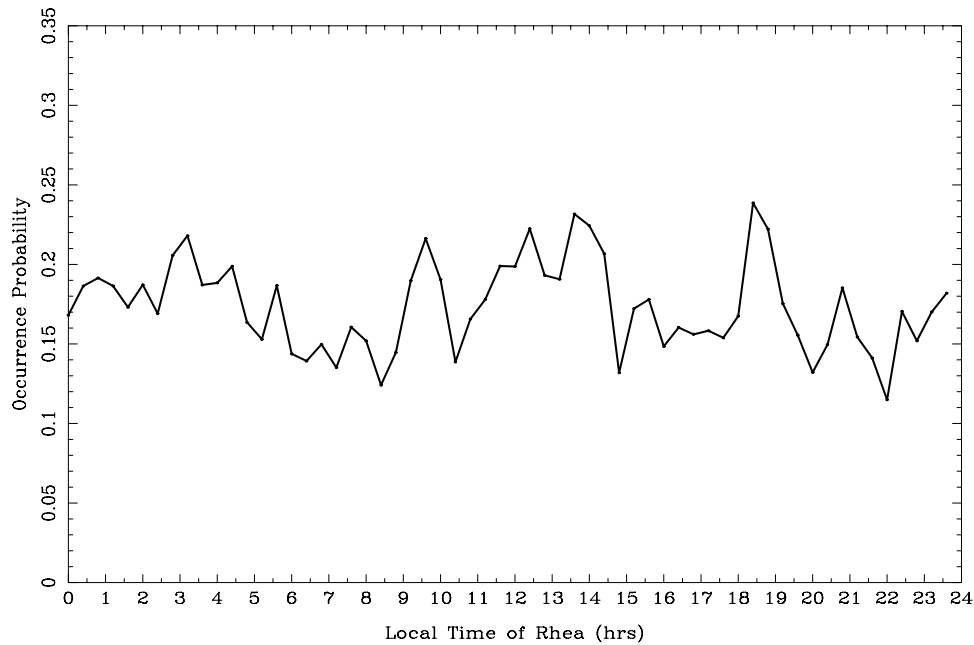


Figure 13. Plot of OP averaged over the range $10^\circ < \text{SSSL} < 180^\circ$ versus Rhea LT.

enlarging the size of bins in orbital phase of Rhea from 6 degrees to 30 degrees (dashed curve of Figure 11). We do not change the size of the bin in SKRLS. Performing the z-test, assuming the subject bin is centered at 282 degrees of orbital phase, we find that this bin is statistically significant relative to all other bins except the two adjacent bins centered at 222 and 252 degrees. However, no bin is statistically significant relative to all the other bins.

[19] At Jupiter, the Io-dependent emission, triggered by Alfvén waves propagating toward Jupiter along the Io flux tube, typically shows higher occurrence probability of emission in two zones of satellite phase, one near 90° and the other near 250° (i.e., the Io-B and Io-C emissions). These zones are due to the radio emission emanating from a broad emission cone with source at low-altitudes (near the gyroresonance point) along the Io magnetic flux tube [Goldstein and Goertz, 1983, Figure 1 and Figure 9.7]. We would thus expect an increase in OP at Cassini for two orbital phases separated by about 180° . Emission from only one orbital phase near 290° (as observed for Rhea in Figure 11) is not obviously explainable by this model unless there is a quenching or obscuring mechanism for emission when Rhea is near an orbital phase of 90° .

6. Summary and Conclusions

[20] We have used the new SKR longitude system based on a variable period as presented by Kurth *et al.* [2007]. This new system has organized the radio emission data and allows us to investigate influence of the occurrence probability of SKR on Saturnian moons. The data have been analyzed for all frequencies of the SKR and for times from 18 June 2004 to 29 June 2006 inclusive.

[21] Our results indicate a statistically meaningful increase in the occurrence probability of SKR when Titan is located near a local time of midnight ($21 \text{ hours} < \text{LT} < 3 \text{ hours}$) in the Saturn magnetotail, and a decrease of SKR occurrence

probability when Titan is in the afternoon sector ($12 \text{ hours} < \text{LT} < 18 \text{ hours}$). If we are to assume that the source is on the dayside of Saturn, as is believed for most SKR, then Titan's presence in the magnetotail influences the source of SKR on the opposite side of Saturn. From the observations of Farrell *et al.* [2005] we know, however, that at least some SKR has a source on the nightside of Saturn. This region would be inside Titan's orbit, near local time 12 hours, on field lines in the range $10 < L < 15$.

[22] If the emission mechanism were the same as that proposed for Io-dependent emission of decametric emission at Jupiter, then we would expect emission that shows some symmetry relative to the orbital phase of Titan, just as occurs for Io. However, we believe the increase of OP for particular ranges of orbital phase seen in Figures 2 and 3 is coincidental due to the clock-like nature of Saturnian radio emission reported for Voyager results. This is because the Cassini orbit during the observations reported has been constrained primarily to the morning sector. Figures 4, 5, and 9 show significant increases in OP when Titan is near a local time of midnight. The influence of Titan on the occurrence probability of SKR is significant, based on our statistical results. This is distinct from the possible influence of Titan on the occurrence of substorms within the Saturnian magnetosphere. At this point we only speculate on the physical mechanism by which Titan influences the generation of SKR.

[23] The SKR dependence on the local time of Titan is fundamentally different from the mechanism by which Io-dependent emission is generated. In the case of Jupiter, electrons are accelerated along the Io flux tube, subsequently generating radio emission via the cyclotron maser mechanism near the footprint of the flux tube. At Saturn the SKR OP increases relative to the LT of Titan and there are probably no large densities of electrons streaming along the Titan flux tube toward Saturn.

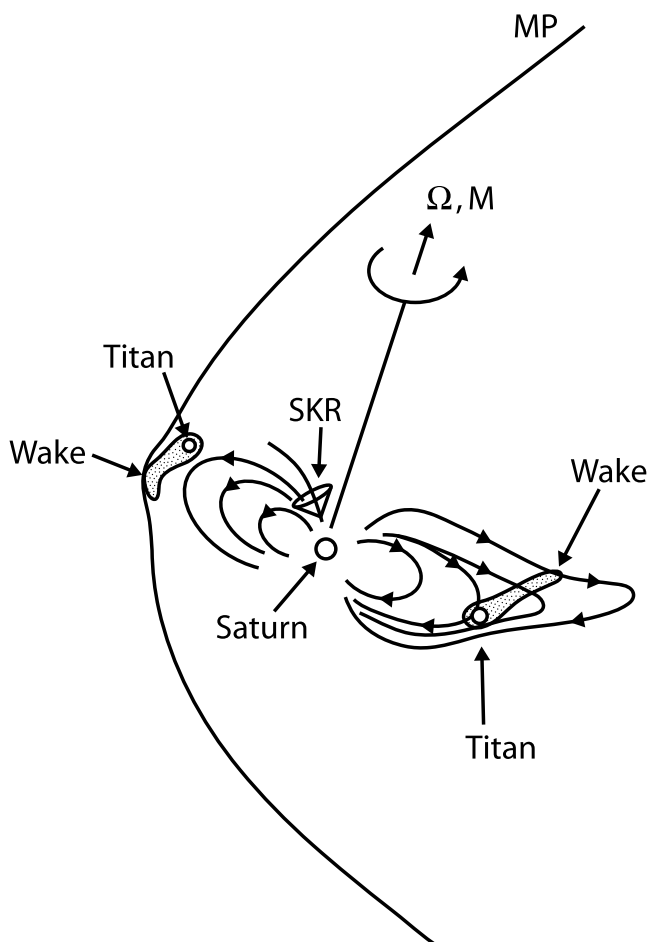


Figure 14. Cartoon depicting Titan and its extensive wake as seen both in the magnetotail (as a source of plasma for newly reconnecting field lines) and on the dayside (producing a distortion of the local magnetopause position).

[24] We hypothesize that Titan's presence in the magnetotail may contribute to the efficiency of reconnection and/or may increase the rate of plasma transport onto reconnected field lines that map to the auroral region and active SKR generation sites. We do know that Titan is a significant source of pick-up ions and mass loading [cf. Mitchell *et al.*, 2005; Szego *et al.*, 2005] and has weak Alfvén wings (relative to Jupiter's Io) but an extensive wake [cf. Neubauer *et al.*, 2006; Ma *et al.*, 2006]. We speculate that perhaps the ions associated with the wake of Titan may participate in reconnection events within the magnetotail, thus enhancing any subsequent plasma precipitation to the Saturn ionosphere. This would suggest a possible nightside source for some of the SKR, however, within 2 hours any such precipitation initiated within the magnetotail would corotate to the dayside where it may enhance the generation of SKR within the known source region.

[25] We observe a diminution of SKR when Titan is located in the approximate range 12 hours < LT < 18 hours. We hypothesize that at least on occasion Titan and its wake in this region disrupts the normal reconnection process and thus prevents plasma entry into the Saturnian magnetosphere and consequent generation of SKR. We speculate

that since Titan often comes near to the dayside magnetopause, the wake plasma may somehow inhibit or decrease the efficiency of the reconnection process (in contrast to the nightside) and thereby decrease the current to the dayside SKR source region. Perhaps the plasma pressure associated with the wake of Titan locally distorts the location of the magnetopause (reconnection site). We note the plasma and magnetic pressure in the Titan wake [see Neubauer *et al.*, 2006, Table 4] are larger than the model dynamic pressure at Saturn's magnetopause [cf. Arridge *et al.*, 2006]. In Figure 14 we show a cartoon indicating Titan and its wake providing a source of ions for reconnecting field lines in the magnetotail and perhaps disrupting reconnection on the dayside. The mechanism for this quenching as well as the details of the mechanism by which Titan influences reconnection in the magnetotail await further investigation by MHD or multifluid calculations.

[26] There is a secondary increase in OP of SKR in the local time range 8 hours < LT < 10 hours. This increase may be associated with the location of Cassini during the data sampling. The apoapsis of the Cassini orbit was centered near 8–9 hours of local time for the time period prior to November 2006, before it precessed clockwise to earlier local times.

[27] The results for Rhea are not conclusive. The marginally significant increase in OP for Rhea is observed only in orbital phase (280°–295°) but not in local time. This would imply emission associated with the location of Rhea relative to the observer. The results are not similar to those of Io-dependent emission at Jupiter, however, because we apparently are only observing satellite-dependent emission near eastern elongation but not western elongation as we would also expect. One explanation may be that “Rhea-dependent” emission is very temporal in nature. At this time we consider the observations of Rhea marginal, and further study is required.

[28] **Acknowledgments.** We thank J. Hospodarsky for clerical assistance and C. Piker for programming support. This work was supported by Jet Propulsion Laboratory contract 1279973 to the University of Iowa.

[29] Amitava Bhattacharjee thanks the reviewers for their assistance in evaluating this paper.

References

- Arridge, C. S., N. Achilleos, M. K. Dougherty, K. K. Khurana, and C. T. Russell (2006), Modeling the size and shape of Saturn's magnetopause with variable dynamic pressure, *J. Geophys. Res.*, *111*, A11227, doi:10.1029/2005JA011574.
- Bigg, E. K. (1964), Influence of the satellite Io on Jupiter's decametric emission, *Nature*, *203*, 1008–1010.
- Boischoit, A., A. Lecacheux, M. L. Kaiser, M. D. Desch, and J. K. Alexander (1981), Radio Jupiter after Voyager: An overview of the planetary radio astronomy observations, *J. Geophys. Res.*, *86*, 8213–8226.
- Burke, B. F., and K. L. Franklin (1955), Observations of a variable radio source associated with the planet Jupiter, *J. Geophys. Res.*, *60*, 213–217.
- Carr, T. D., M. D. Desch, and J. K. Alexander (1983), Phenomenology of magnetospheric radio emissions, in *Physics of the Jovian Magnetosphere*, edited by A. J. Dessler, pp. 226–284, Cambridge Univ. Press, Cambridge, U. K.
- Clarke, J. T., et al. (2005), Morphological differences between Saturn's ultraviolet aurorae and those of Earth and Jupiter, *Nature*, *433*, 717–719.
- Crary, F. J. (1997), On the generation of an electron beam by Io, *J. Geophys. Res.*, *102*, 37–49.
- Desch, M. D., and M. L. Kaiser (1981), Saturn's kilometric radiation: Satellite modulation, *Nature*, *292*, 739–741.
- Ergun, R. E., Y.-J. Su, F. Bagenal, and P. A. Delamere (2002), Recent M-I coupling discoveries and how they apply to the outer planets, paper

- presented at Magnetospheres of Outer Planets Meeting, Johns Hopkins Univ. Appl. Phys. Lab., Laurel, Md.
- Farrell, W. M., M. D. Desch, M. L. Kaiser, A. Lecacheux, W. S. Kurth, D. A. Gurnett, B. Cecconi, and P. Zarka (2005), A nightside source of Saturn's kilometric radiation: Evidence for an inner magnetosphere energy driver, *Geophys. Res. Lett.*, **32**, L18107, doi:10.1029/2005GL023449.
- Goldreich, P., and D. Lynden-Bell (1969), Io, a Jovian unipolar inductor, *Astrophys. J.*, **156**, 59–78.
- Goldstein, M. L., and C. K. Goertz (1983), Theories of radio emissions and plasma waves, in *Physics of the Jovian Magnetosphere*, edited by A. J. Dessler, pp. 317–352, Cambridge Univ. Press, Cambridge, U. K.
- Gurnett, D. A., W. S. Kurth, and F. L. Scarf (1981), Plasma waves near Saturn: Initial results from Voyager 1, *Science*, **212**, 235–239.
- Gurnett, D. A., et al. (2004), The Cassini radio science investigation, *Space Sci. Rev.*, **114**, 395–463.
- Hansen, K. C., A. J. Ridley, G. B. Hospodarsky, N. Achilleos, M. K. Dougherty, T. I. Gombosi, and G. Toth (2005), Global HD simulations of Saturn's magnetosphere at the time of Cassini approach, *Geophys. Res. Lett.*, **32**, L20S06, doi:10.1029/2005GL022835.
- Hartle, R. E., et al. (2006), Preliminary interpretation of Titan plasma interaction as observed by the Cassini Plasma Spectrometer: Comparisons with Voyager 1, *Geophys. Res. Lett.*, **33**, L08201, doi:10.1029/2005GL024817.
- Higgins, C. A., J. D. Menietti, and I. W. Christopher (2006), Europa control of Jovian radio emission: A Galileo study, *Geophys. Res. Lett.*, **33**, L14110, doi:10.1029/2006GL026218.
- Kaiser, M. L., and M. D. Desch (1982), Saturnian kilometric radiation: Source locations, *J. Geophys. Res.*, **87**, 4555–4559.
- Kaiser, M. L., M. D. Desch, and A. Lecacheux (1981), Saturnian kilometric radiation: Statistical properties and beam geometry, *Nature*, **292**, 731–733.
- Kaiser, M. L., M. D. Desch, W. S. Kurth, A. Lecacheux, F. Genova, B. M. Pedersen, and D. R. Evans (1984), Saturn as a radio source, in *Saturn*, edited by T. Gehrels and M. S. Matthews, pp. 378–415, Univ. of Ariz. Press, Tucson, Ariz.
- Kurth, W. S., D. A. Gurnett, and F. L. Scarf (1981), The control of Saturn's kilometric radio emission by Dione, *Nature*, **292**, 742–745.
- Kurth, W. S., et al. (2005), An Earth-like correspondence between Saturn's auroral features and radio emission, *Nature*, **433**, 722–725.
- Kurth, W. S., A. Lecacheux, T. F. Averkamp, J. B. Groene, and D. A. Gurnett (2007), A Saturnian longitude system based on a variable kilometric radiation period, *Geophys. Res. Lett.*, **34**, L02201, doi:10.1029/2006GL028336.
- Lecacheux, A., and F. Genova (1983), Source location of Saturnian kilometric radio emission, *J. Geophys. Res.*, **88**, 8993–8998.
- Ma, Y., A. F. Nagy, T. E. Cravens, I. V. Sokolov, K. C. Hansen, J.-E. Wahlund, F. J. Crary, A. J. Coates, and M. K. Dougherty (2006), Comparisons between MHD model calculations and observations of Cassini flybys of Titan, *J. Geophys. Res.*, **111**, A05207, doi:10.1029/2005JA011481.
- Mauk, B. H., B. J. Anderson, and R. M. Thorne (2002), Magnetosphere-ionosphere coupling at Earth, Jupiter, and beyond, in *Atmospheres in the Solar System: Comparative Aeronomy*, *Geophys. Monogr. Ser.*, vol. 130, edited by M. Mendillo, A. Nagy, and J. H. Waite, pp. 97–114, AGU, Washington, D. C.
- Mendenhall, W. (1987), *Introduction to Probability and Statistics*, 7th ed., pp. 347–396, PWS-Kent Publ., Boston, Mass.
- Menietti, J. D., J. L. Green, N. F. Six, and S. Gulkis (1987), Ray tracing of Jovian decametric radiation from southern and northern hemisphere sources: Comparison with Voyager observations, *J. Geophys. Res.*, **92**, 27–38.
- Mitchell, D. G., et al. (2005), Energetic ion acceleration in Saturn's magnetotail: Substorms at Saturn?, *Geophys. Res. Lett.*, **32**, L20S01, doi:10.1029/2005GL022647.
- Neubauer, F. M. (1980), Nonlinear standing Alfvén wave current system at Io: Theory, *J. Geophys. Res.*, **85**, 1171–1178.
- Neubauer, F. M., D. A. Gurnett, J. D. Scudder, and R. E. Hartle (1984), Titan's magnetospheric interaction, in *Saturn*, edited by T. Gehrels and M. S. Matthews, pp. 760–787, Univ. of Ariz. Press, Tucson, Ariz.
- Neubauer, F. M., et al. (2006), Titan's near magnetotail from magnetic field and electron plasma observations and modeling: Cassini flybys TA, TB, and T3, *J. Geophys. Res.*, **111**, A10220, doi:10.1029/2006JA011676.
- Sittler, E. C., Jr., et al. (2006), Energetic nitrogen ions within the inner magnetosphere of Saturn, *J. Geophys. Res.*, **111**, A09223, doi:10.1029/2004JA010509.
- Su, Y.-J., R. E. Ergun, F. Bagenal, and P. A. Delamere (2003), Io-related Jovian auroral arcs: Modeling parallel electric fields, *J. Geophys. Res.*, **108**(A2), 1094, doi:10.1029/2002JA009247.
- Szego, K., et al. (2005), The global plasma environment of Titan as observed by Cassini plasma spectrometer during the first two close encounters with Titan, *Geophys. Res. Lett.*, **32**, L20S05, doi:10.1029/2005GL022646.
- Warwick, J. W., et al. (1979a), Voyager 1 planetary radio astronomy observations near Jupiter, *Science*, **204**, 955–998.
- Warwick, J. W., et al. (1979b), Planetary radio astronomy observations from Voyager 2 near Jupiter, *Science*, **206**, 991–995.
- Warwick, J. W., et al. (1981), Planetary radio astronomy observations from Voyager 1 near Saturn, *Science*, **212**, 239–243.
- Warwick, J. W., D. R. Evans, J. H. Romig, J. K. Alexander, M. D. Desch, M. L. Kaiser, M. Aubier, Y. Leblanc, A. Lecacheux, and B. M. Pedersen (1982), Planetary radio astronomy observations from Voyager 2 near Saturn, *Science*, **215**, 582–587.
- Wilkinson, M. H. (1989), Io-related Jovian decametric arcs, *J. Geophys. Res.*, **94**, 11,777–11,970.

T. F. Averkamp, J. B. Groene, D. A. Gurnett, G. B. Hospodarsky, W. S. Kurth, and J. D. Menietti, Department of Physics and Astronomy, University of Iowa, Iowa City, IA 52242, USA. (john-menietti@uiowa.edu)
P. Zarka, Observatoire de Paris, Meudon, F-92195 France.